

Experimental and theoretical evidences for the ice regime in planar artificial spin ices

R. P. Loreto,¹ F.S. Nascimento,² R. S. Goncalves,¹ J. Borme,³ J. C. Cezar,⁴ C. Nisoli,⁵ A. R. Pereira,^{1,*} and C.I.L. de Araujo^{1,†}

¹Laboratory of Spintronics and Nanomagnetism (LabSpiN), Departamento de Física, Universidade Federal de Viçosa, 36570-000 - Viçosa - Minas Gerais - Brazil.

²Departamento de Física, Universidade Federal de Ouro Preto, 35931-008 - João Monlevade - Minas Gerais - Brazil.

³INL-International Iberian Nanotechnology Laboratory, 4715-330, Braga, Portugal

⁴Laboratório Nacional de Luz Síncrotron-LNLS, CP 6192, 13083-970 Campinas, Brazil

⁵Theoretical Division and Institute for Materials Science,

Los Alamos National Laboratory, Los Alamos, New Mexico 87545, USA

(Dated: March 1, 2022)

In this work, we explore a kind of geometrical effect in the thermodynamics of artificial spin ices (*ASI*). In general, such artificial materials are athermal. Here, We demonstrate that geometrically driven dynamics in *ASI* can open up the panorama of exploring distinct ground states and thermally magnetic monopole excitations. It is shown that a particular *ASI* lattice will provide a richer thermodynamics with nanomagnet spins experiencing less restriction to flip precisely in a kind of rhombic lattice. This can be observed by analysis of only three types of rectangular artificial spin ices (*RASI*). Denoting the horizontal and vertical lattice spacings by a and b , respectively, then, a *RASI* material can be described by its aspect ratio $\gamma \equiv a/b$. The rhombic lattice emerges when $\gamma = \sqrt{3}$. So, by comparing the impact of thermal effects on the spin flips in these three appropriate different *RASI* arrays, it is possible to find a system very close to the ice regime.

INTRODUCTION

Arrays of nanomagnets designed to resemble the spin ice materials (disordered magnetic states) are known as artificial spin ices (*ASI*). Nowadays, with the advances of the nanotechnology and nanofabrication, *ASI* systems have become so famous as well as their natural counterparts, with the advantage that they can be constructed with desirable geometries and properties. The first *ASI* was built in 2006 and it consists of a two-dimensional ($2d$) square array of 80,000 elongated magnetic nanoislands, each a few hundred nanometers long[1]. The net magnetic moment (spin) of each individual nanoisland is aligned parallel to its longest axis (like in a bar magnet), and is coupled to all other nanoislands of the planar array by the ubiquitous dipolar interaction. Then, in its original configuration, *ASI* tiles a square lattice of vertices, with four nanoislands meeting at each vertex.

The ground state of the artificial square ice obeys the ice rule, which remains the familiar two-in, two-out (two spins must point in, while the other two must point out in each vertex). However, in two dimensions, the standard ice rule is no longer degenerate[1–3]. In addition, *ASI* systems have long been athermal (these compounds were almost always found in frozen at room temperature), until the most recent investigations on patterned ultrathin magnetic films could pave the way to explore and visualize the real-time dynamics of all kinds of different frustrated geometries. Indeed, recently, several works have given attention to certain thermal properties

of *ASI* compounds in diverse types of planar lattices[4–12]. However, the $2d$ lattice obeying the usual two-in, two-out ice rule with a degenerated ground state did not deserve yet an adequate treatment. In this paper, we would like to do this by comparing arrays that exhibit different ground states, when they are heated to a high temperature regime (we mean by high temperature, the practical values in the range $300K - 800K$). Some of their magnetic properties (as a function of temperature T) are observed by Photoemission Electron Microscopy (*PEEM*) combined with *X*-ray Magnetic Circular Dichroism (*XMCD*) measurements. *MOKE* signals are also analyzed. It is done by deforming continuously the square lattice in a rectangular one. Therefore, we experimentally focus on rectangular artificial spin ices (*RASI*) with horizontal and vertical lattice parameters given by a and b respectively (b is kept constant while a is varied). Our samples match in three classes of *RASI*, appropriately designed to illustrate how a particular planar system can approximate of the ice regime. They are heated from room temperature until a temperature near $800K$ (just below the Curie Temperature of the permalloy, which is $T_C = 873K$).

Theoretical calculations[13] concerning the rectangular artificial systems suggest that the ice regime (with the required degenerate ground state), could be observed when the aspect ratio of the lattice ($\gamma \equiv a/b$) is equal to $\sqrt{3}$ (the rhombic lattice). On the other hand, like the artificial square array, the ground states of *RASI* compounds with $1 < \gamma < \sqrt{3}$ and $\gamma > \sqrt{3}$ are not degenerate, but they have very distinct magnetic properties: in the first case ($1 < \gamma < \sqrt{3}$), there are residual magnetic charges at each vertex, alternating from positive to negative along the neighbor vertices (these charges are not

* apereira@ufv.br.

† dearaujo@ufv.br

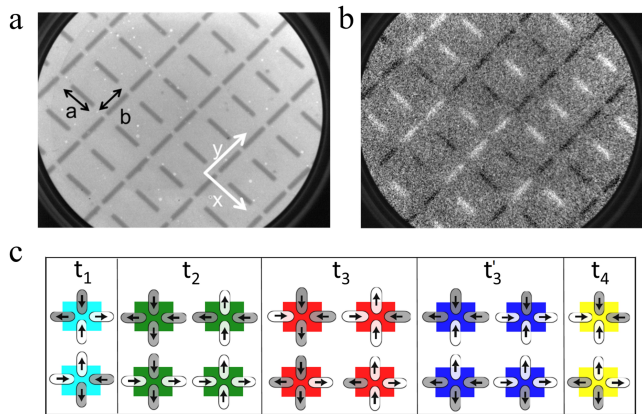


Figure 1. (a) $30\mu\text{m} \times 30\mu\text{m}$ PEEM image of $\gamma = \sqrt{3}$ RASI lattice. The Permalloy nanoislands have $2800\text{nm} \times 400\text{nm} \times 10\text{nm}$. It would be useful to say that those nanomagnets, larger than usual ASI systems, were used in order to achieve higher image contrast in our PEEM, after careful tests performed by micromagnetic simulations and Magnetic Force Measurements, which ensured that it is inside the limit to present monodomains (not supporting vortices or multidomains). (b) Typical XMCD measurement for the same area of (a) with the clear and dark contrast representing the orientation of the islands monodomains, in each direction. The measurement was taken with the array rotated 45 degrees from the X-ray sensitivity to resolve x and y direction at the same time. (c) Possible vertex types for each vertex represented by different colors, where arrows represent the orientation of the island related to XMCD pattern.

cylindrically symmetric exhibiting a strong quadrupole moment). This system can be characterized as anti-ferromagnetic (along the vertical and horizontal lines of spins). In the second case ($\gamma > \sqrt{3}$), there are alternating residual magnetic moments along the neighbor vertices. Again, looking the vertical and horizontal lines of spins, it can be characterized as a ferromagnetic state. At $\gamma = \gamma_R = \sqrt{3}$, these two distinct types of states have the same energy and the ground state becomes degenerated. This special case separates the antiferromagnetic state ($1 < \gamma < \sqrt{3}$) from the ferromagnetic one ($\gamma > \sqrt{3}$) and can be distinguished as a more realistic spin ice state in these artificial systems (later, the difficulty of obtaining an accurate ice state, theoretically and experimentally, will be discussed).

Figure 1a shows an image of a RASI with $\gamma = \sqrt{3}$ obtained by PEEM measurements combined with XMCD technique (see also Fig. 1b), displaying the magnetic monodomains of the nanoislands. Figure 1c shows the five possible vertex types of these structures. Vertex types t_1 and t_2 obey the ice rule (two-in, two-out) while the other three (t_3 , t'_3 and t_4) represent excited states singly (t_3 and t'_3) and doubly (t_4) charged magnetic monopoles[13]. The energy of all these vertex types depends on γ . For $\gamma = \gamma_R$, the t_1 and t_2 types have the same energy, yielding to a degenerate ground state. To easier

see such an array, it is better to replace the net magnetic moment of the nanoislands by a point-like dipole at their centers. Then, the four dipoles (spins) for the case $\gamma = \sqrt{3}$ are located at the vertices of a rhombus with short and long diagonals b and $a = \sqrt{3}b$, respectively and, therefore, they are equidistant (in this case, the distance of each pair of spins in a rhombus is b). Then, we can say that the spins are placed at the vertices of a kind of rhombic lattice with rhombi having spins pointing out parallel to their diagonals alternating (along the diagonal of the rectangles) with rhombi having spins pointing out perpendicular to their diagonals. A rhombic lattice is one of the five $2d$ lattice types as given by the crystallographic restriction theorem.

Here, we show theoretically and experimentally that the geometry distortion of the planar arrays may be an additional ingredient able to cause important physical phenomena in ASI materials. In fact, by studying three RASI systems with different aspect ratios γ , we demonstrate that the geometrical influence goes beyond the simple effect of the variation of the lattice parameters. To explain the aims of this work, we organize the sequence of the paper as follows: firstly, we use Monte Carlo (MC) simulations to calculate the specific heat and topologies density as functions of temperature T . In principle, based on the square lattice, these thermodynamic quantities have important features only when the temperature scale is on the order of $10^4 K$. If it is true, most of these theoretical results could not be experimentally verified but they will give us, at least, interesting insights about ASI and RASI. On the other hand, our MC simulations also suggest that the critical temperatures for the specific heat fall rapidly as γ increases till $\sqrt{3}$, guiding some possibilities and questions about RASI that only experiments could answer. Hence, an experimental investigation is the second natural step of this paper. We then experimentally measure the magnetization and topology density as functions of T by heating the samples from room temperature ($300K$) to $\sim 750K$. Although this range of temperature is about (10 – 100) times smaller than the typical temperature scale necessary to easily flip the large spin of the magnetic nanoislands, we can directly observe very interesting thermal effects in some artificial materials, when the geometry is stretched from the square to the rectangular lattice. The main conclusion here is that arrays with $\gamma \approx 1$ (almost square) are essentially athermal systems as already mentioned in several works, while arrays with $\gamma \approx \sqrt{3}$ present important thermal and dynamical effects even at a temperature scale on the order of $10^2 - 10^3 K$. We will see that this effect does not have to do with the fact that the rectangular arrays (with $\gamma > 1$) are more weakly coupled than the square array (of side b). Really, although the temperature-induced onset of magnetic fluctuations increases with the lattice spacing and related interaction strength between nanoislands[8], our results show that an extra factor will be more fundamental here: lattice geometry. A purely geometrical effect will make the net

RESULTS

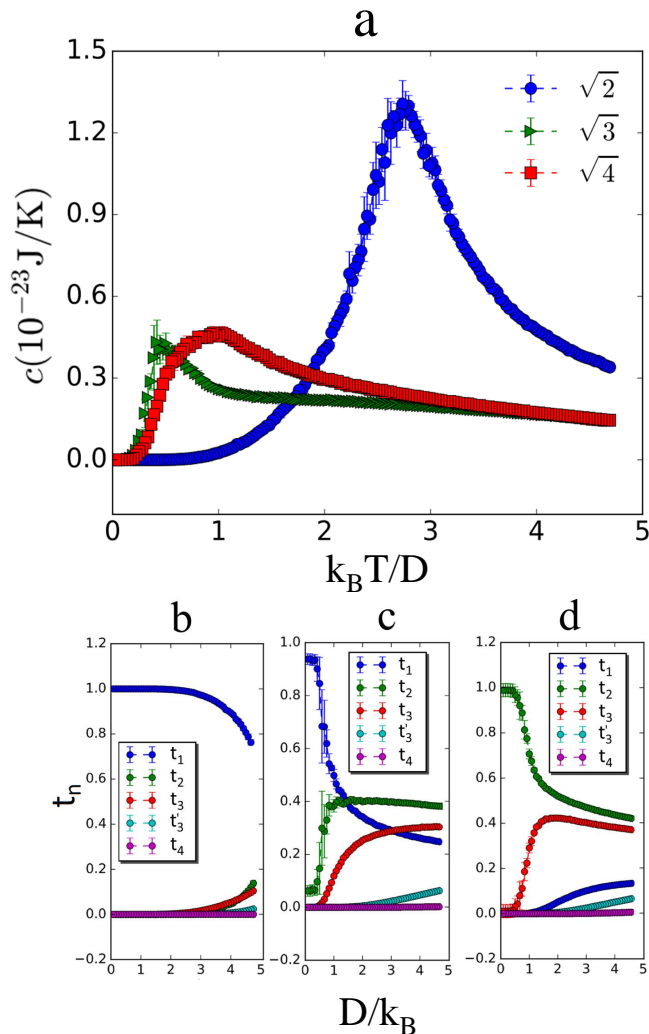


Figure 2. (a) Specific heat of *RASI* with different values of γ obtained by Monte Carlo simulations. Parts (b), (c) and (d) show the density of states for each vertex type (t_1, t_2, t_3, t_4 and t_4) in the lattices with $\gamma = \sqrt{2}$, $\gamma = \sqrt{3}$ and $\gamma = \sqrt{4}$ respectively, as a function of temperature.

magnetic moments to appear flexible enough to rather flip with a smaller amount of effort (for temperatures compatible with artificial magnets), allowing the dipolar interaction to have more protagonism in determining the dynamical properties of the system than usually it does. For investigating the two aims cited above, *RASI* materials with aspect ratios equal to $\gamma = \sqrt{2}$, $\gamma = \gamma_R = \sqrt{3}$ and $\gamma = \sqrt{4}$ were appropriately chosen and fabricated. So the effects proposed here will be exposed by comparing some thermodynamic quantities of these three rectangular arrays, observing the roles of their geometries.

We start by reporting the thermodynamic results for *RASI* as obtained by *MC* simulations. The calculations presented here use the point-dipole approximation but we have also done calculations using the dumbbell model. We did not find any relevant differences between the two methods. The model is implemented by standard *MC* techniques on a system with $N = 364$ spins. Here, the spin-spin interaction is assumed to be purely dipole-dipole such that the Hamiltonian is given by $H = D \sum_{i>j} \left[\frac{\hat{e}_i \cdot \hat{e}_j}{r_{ij}^2} - \frac{3(\hat{e}_i \cdot \vec{r}_{ij})(\hat{e}_j \cdot \vec{r}_{ij})}{r_{ij}^5} \right] s_i s_j$, where $D \approx 2.1 \times 10^{-19} \text{ J}$ is the coupling constant of the dipolar interaction, \hat{e}_i is the local Ising axes of the rectangular lattice, r_{ij} is the distance between spins and $s_i = \pm 1$ represents the two states (up/down) of the Ising spin. In our procedure, Monte Carlo step consists of N single-spin flips and we have used 10^4 Monte Carlo steps to reach equilibrium configurations and 10^5 steps to get thermodynamics averages. Samples are first prepared in a disordered state and then cooled to low temperatures; this annealing protocol in general drives the spin configuration to the ground state. In this process, the specific heat is calculated by the fluctuations in the total energy of the system, $c = (\Delta E)^2 / k_B T^2 N$.

For the usual artificial square ice, previous calculations by Silva *et al.*[5] have suggested the existence of a phase transition at a critical temperature $T_P \sim 7.2D/k_B$, where D is the coupling constant of the dipolar interaction and k_B is the Boltzmann constant. Really, the specific heat exhibits a sharp peak at T_P , whereas the amplitude diverges logarithmically with the system size L . Such a phase transition was speculated to be attributed to the vanishing of the string tension joining monopoles of opposite charges: below T_P , the monopoles are joined by an energetic (and observable) string (Nambu monopoles[15]); above T_P , the string tension should vanish and some monopoles become free to move (actually, they may not be completely free because a monopole pair is subjected to an entropic force that exhibits, in two dimensions, a logarithmic distance dependence[5, 16]). Concerning the specific heat, our *MC* calculations lead to similar behaviors for the *RASI* materials. Figure 2 shows the specific heat as a function of temperature for the three different cases considered here. As expected, the critical temperature ($T_{\sqrt{n}}$, $n = 2, 3, 4$), at which the peaks occur, is a function of the aspect ratio γ . Initially, as γ is increased from 1 (square ice), the critical temperature decreases. It is expected because the coupling among nanoislands becomes weaker as the array becomes more stretched. However, interestingly, this critical temperature has a minimum for $\gamma = \sqrt{3}$, in such a way that $T_P > T_{\sqrt{2}} > T_{\sqrt{3}} < T_{\sqrt{4}} < T_{\sqrt{2}}$. Except for $\gamma = \sqrt{3}$, the reasonable idea that the critical temperature decreases as γ increases works very well ($T_{\sqrt{2}} = 2.7D/k_B$, $T_{\sqrt{3}} = 0.5D/k_B$ and $T_{\sqrt{4}} = 0.8D/k_B$) see Fig. 2a). It reinforces the fact that a rhombic ice has special properties

as demonstrated by previous calculations[13]. Indeed, to our knowledge, it is the only one planar case, obeying the familiar two-in, two-out ice rule, that has a degenerate ground state (topologies t_1 and t_2 possess the same energy). In these circumstances, the string tension should be zero for any temperature (including the absolute zero). However, an entropic effect generates an attractive interaction potential ($T \ln R$, where R is the distance between a monopole and its antimonopole in a pair) in such a way that monopoles should become free only at $T = 0$. For finite temperatures, they may be found apart but not completely free. To try to observe some vestiges of the geometry features, we have also calculated the topology densities as functions of temperature. These results are shown in Figs.2b, 2c and 2d. The rectangular ice magnets with $\gamma = \sqrt{2}$ and $\gamma = \sqrt{4}$ start (at $T = 0$) with all vertices in their respective natural ground states (the vertex types t_1 and t_2 , respectively). On the other hand, the rhombic ice ($\gamma_R = \sqrt{3}$) starts with all vertices in the vertex type t_1 , which may be merely one of its possible ground states. In all situations, as T is increased from zero, the other vertex types start slowly to arise around the lattice. It occurs in different manners as γ changes. For $\gamma = \sqrt{2}$, the system practically remains entirely in its ground state for a large range of temperatures, in such a way that, the vertex type t_1 begins to really decrease only for $T > 3D/k_B$ (Fig.2b). Like the square ice, this high temperature value for the materialization of excitations indicates that systems with relatively small aspect ratio ($\gamma \approx 1$) tend to be athermal (in the context frequently used in the literature for *ASI*). Conversely, for the special case of a rhombic lattice, the initial state (with all vertices in t_1) reduces rapidly as T increases and, simultaneously, the density of the t_2 vertex type increases considerably (similar results are obtained if the initial state would have all vertices in t_2 , which is also a possible ground state in this case). It suggests an immediate activity in the spin fluctuations, even at relatively low temperatures. Note that the density of the ground state vertex types (t_1 and t_2) becomes exactly equal just at the critical temperature $T_{\sqrt{3}}$ (see Fig.2c). Only these two vertex types are essentially fluctuating for low T . It means that, for $0 < T < T_{\sqrt{3}}$, the system still persists almost entirely in its ground states (t_1 and t_2 have the same energy when $\gamma = \sqrt{3}$), since the vertex types t_3, t'_3 and t_4 were not significantly excited yet. Indeed, for this particular case, any mixture of the states t_1 and t_2 , if it is possible to occur, would also be a ground state. Therefore, as the density of t_2 increases (and the density of the excited states t_3, t'_3 and t_4 remains close to zero), this degenerate system seems to be accessing several of its different ground states. For $T > T_{\sqrt{3}}$, the vertex types t_3 and t'_3 start to be excited and then, this upper temperature phase rather signalizes the emergence of monopoles with tensionless strings. Finally, Fig.2d shows that the case $\gamma = \sqrt{4}$ has a behavior qualitatively similar to the first example studied here ($\gamma = \sqrt{2}$). The basic differences are the ground states

and the fact that the t_3 monopoles (red circles) are more easily excited in the array with $\gamma = \sqrt{4}$, producing a lower transition temperature. The expressive presence of the t_3 monopoles in comparison with the t'_3 monopoles (in all cases) is justified because they have smaller energy (actually, the difference between the energy of t'_3 and t_3 vertex types increases as γ increases[13]). The above theoretical calculations are very suggestive: $T_{\sqrt{3}}$ is about 15 times smaller than T_P , which means that the rhombic ice exhibits, at much lower temperatures, a richer dynamics than the square ice. Moreover, it is not only due to a larger mean distance among the magnetic nanoislands, but mainly, due to the lattice geometry itself since the *RASI* with $\gamma = \sqrt{4}$ presents less fluctuations than the artificial rhombic lattice. Therefore, *RASI* materials deserve a deeper investigation from the experimental point of view. This is a natural next step: the study of high temperature *RASI*. Here, high temperature means the practical range in the interval $300K < T < 800K$.

With these indicative theoretical results in mind, we now consider realistic experimental arrangements in which the temperature of the three kinds of *RASI* systems varies from $300K$ to $750K$. This range of T is, in principle, about 10 – 100 times smaller than the temperature scale of the most theoretical calculations presented above, but it is below the Curie temperature (T_C) of the permalloy nanoislands.

For the fabrication of Permalloy nanoislands, a multilayer with composition *Si / Ta 3nm / Ni₈₀Fe₂₀ 10nm / Ta 3nm* was previously prepared by sputtering from tantalum (seed and cap layer) and alloyed permalloy target, on silicon substrate. Then, the samples were covered with a $85nm$ layer of *AR-N7520.18* negative tone photoresist and patterned by electron lithography at $100kV$ of acceleration voltage. After development, the samples were etched by ion milling at 20° from normal incidence, using secondary ion mass spectroscopy to detect the end of the process. An ashing in oxygen plasma was subsequently performed to remove the photoresist. The nanoislands dimensions of $l = 2800nm$ and $w = 400nm$ were conceived in order to present magnetic monodomain in each island. The y -axis lattice spacing of $b = 3550nm$ was kept in all samples and the x -axis lattice constant a ranged from $5017 - 7100nm$ in such a way that we have investigated by (*PEEM - XMCD*), *RASI* arrangements with aspect ratios $a/b = \sqrt{2}, \sqrt{3}$ and $\sqrt{4}$ (see Fig. 3). For the *PEEM - XMCD* measurements the samples were heated at different temperatures and images were taken just after temperature switch-off to prevent different sample holder dilatation and beam defocusing. The *MOKE* signal was obtained during sample heating. These systems were built on an area of $100\mu m^2$, which enabled topologies density analysis in arrays of up 10×14 unit cell (280 islands). We have also done some Monte Carlo numerical calculations to compare with experimental results.

The *XMCD* measurements were performed at *PGM* beamline of the Brazilian Synchrotron Light Laboratory

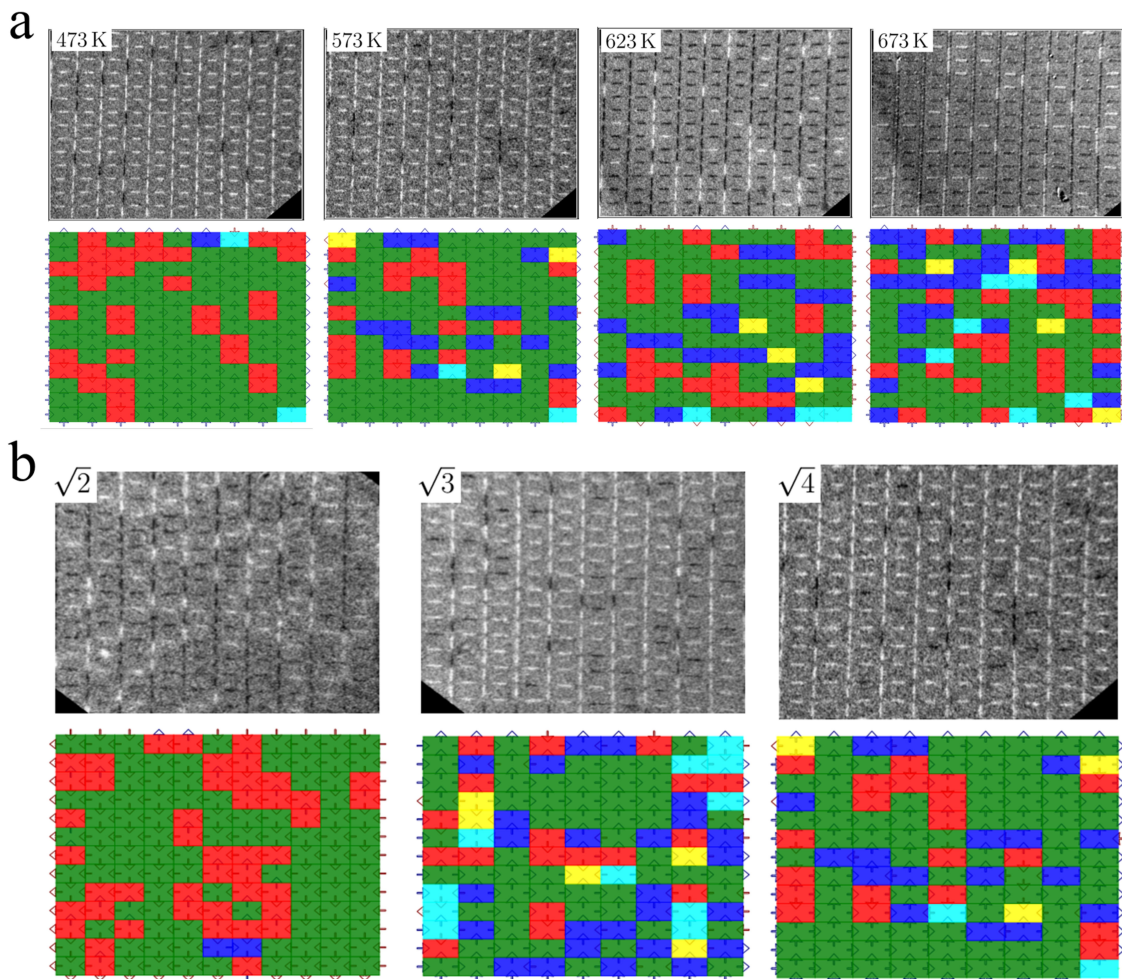


Figure 3. (a) $100 \mu\text{m} \times 100 \mu\text{m}$ PEEM – XMCD images of $\gamma = \sqrt{4}$ RASI for different temperatures (up) and mapped respective magnetic configurations (down). (b) PEEM – XMCD images for $\gamma = \sqrt{2}$, $\gamma = \sqrt{3}$ and $\gamma = \sqrt{4}$ for same temperature of 573K

[?]. They result from the core-level absorption of circularly polarized soft X-ray by a magnetic element and the transfer of right (RCP) or left (LCP) circularly polarized angular momentum of the photons to the excited photoelectrons. The spin and orbital moments can be determined from linear combinations of the dichroic difference intensities of RCP and LCP. The images were taken on the Nickel $L_{2,3}$ edge with a photon energy of 850eV. The islands array was placed rotated 45° related to the X-ray sensitivity in order to fully resolve both x and y directions. MOKE measurements were made using a p -polarized source. The islands array were placed rotated 45° related to the scattering plane to fully resolve both x and y directions. The array was saturated by an external magnetic field and the samples were heated in a low vacuum environment to prevent oxidation. The MOKE signal was recorded by varying the temperature in the sample.

Figure 3a shows a sequence of snapshots of a RASI with $\gamma = \sqrt{4}$. The images were obtained with sam-

ples initially at room temperature (RT) and heated to 473K, 573K, 623K and 673K. The ground state of this array[13] should have all vertices in the vertex type t_1 . Figure 3a shows, more explicitly, how the temperature can actuate to generate fluctuations, creating and destroying all possible low energy excitations into the system (including monopole pairs). Note also that the density of these low energy excitations increases with T . These pictures also demonstrate that most of these excitations are displayed along the vertical direction, since this is the case with less energy[13]. To emphasize and illustrate the role of the thermal effects on the creation of excitations in RASI materials, we investigate experimentally how magnetized samples will be affected as the temperature is increased. Figure 3b presents a comparison of the vertex types for different RASI ratio at the same temperature. Those measurements corroborate the prediction of higher density of high energetic vertex types for the orthorhombic $\gamma = \sqrt{3}$ geometry [14].

All samples were initially prepared (at RT) with nor-

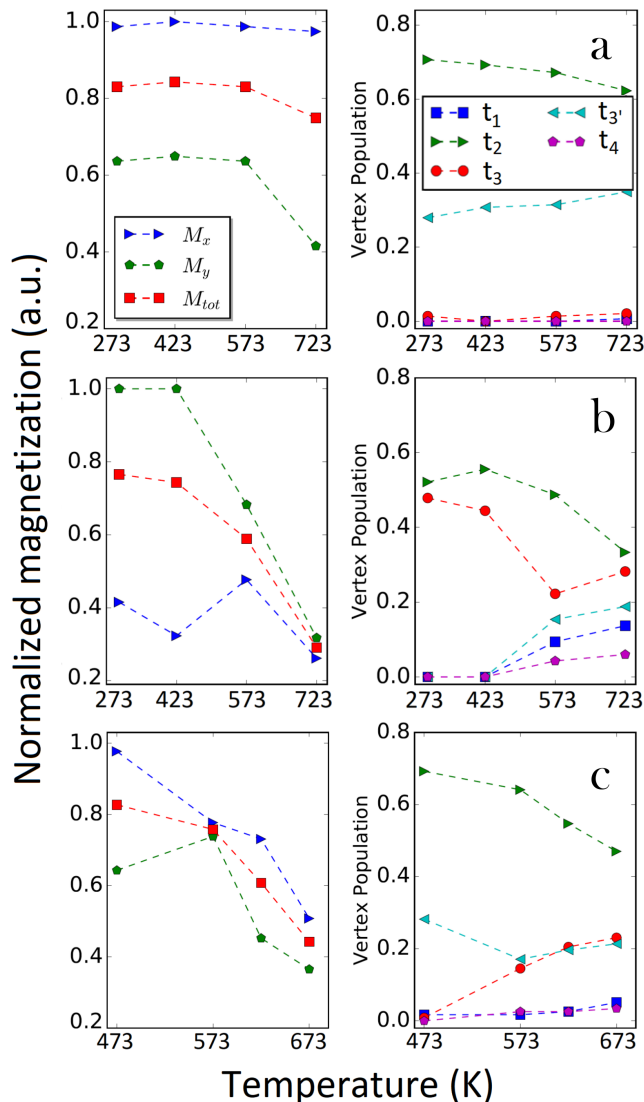


Figure 4. Normalized magnetization and population of vertex types for lattices with (a) $\gamma = \sqrt{2}$, (b) $\gamma = \sqrt{3}$ and (c) $\gamma = \sqrt{4}$. The magnetization and topologies are calculated from the *XMCD* measurements as shown in Fig. 3.

normalized magnetization along lattice diagonal. It was used four values for T . As the temperature is increased, M_{tot} decreases for the three cases but with different behaviors. For instance, Fig.4a shows the Magnetization (left) and the vertex types density (right) for the case $\gamma = \sqrt{2}$ as the temperature is varied from 300K to ~ 750 K. Note that the magnetization decreases very slowly as T increases. Meanwhile, there is a slow increasing of the monopoles number (t_2 and t_3). Such a behavior reveals that this system, like the square ice, is essentially athermal in the range of temperatures compatible with experiments in artificial spin ices. The magnetic moments of the nanoislands do not flip easily and the magnetization remains practically unchanged during all interval of temperatures studied. On the other hand, for the special case

of $\gamma = \sqrt{3}$, the magnetization decreases very rapidly as T increases (left side of Fig.4b) and seems to vanish even at $T < T_C$, while the monopoles population (including also doubly charged monopoles) increases considerably as T increases, mainly for $T > 550$ K (right side of Fig.4b). This example indicates that the geometry may produce favorable conditions to flip the magnetic moments, making the system to exhibit its thermodynamic properties at lower temperatures. To confirm this fact, we have also investigated the case $\gamma = \sqrt{4}$. It suggests that, for $\gamma > \gamma_R$, the magnetization decreases somewhat slower again as T increases (see the left side of Fig.4c), but it falls much more rapidly as compared to the array with $\gamma = \sqrt{2}$. The different temperature range was chosen to better show the magnetization decay region, which is slightly different from the two other previous samples, once in this particular sample the ground state is predicted to be in the ferromagnetic regime. We then notice that the experimental data obtained for the magnetization can be connected with the theoretical calculations for the specific heat: the temperature in which M_{tot} goes to zero and the specific heat presents a peak is a minimum for $\gamma = \sqrt{3}$. These thermodynamical features are caused mainly by geometrical effects, reinforcing the idea that the string tension tends to vanish for the rhombic ice. This lattice is singular since it changes the tendencies in rectangular arrays as γ is increased from 1 (square ice). Indeed, if the lattice were stretched continuously, one expects that the critical temperature should decrease monotonically as γ increases because the mean distance among the nanoislands increases (and as a consequence, the mean coupling among the spins decreases). Of course, it is not the case here. Figure 5 shows the *in-situ MOKE* signal measured as a function of temperature in the lattice diagonal direction, just after magnetization saturation in the same direction. These results also confirm the geometrical deformation effect observed in the *MC* simulations and *XMCD* measurements. The difference in the slope of $\gamma = \sqrt{3}$ curve comes from the fact that the ground state is degenerated and then the saturation, which imply in t_2 vertex type, remains at low temperatures in comparison with the other geometries that favors vertex configuration to ground state or formation of high energy vertex configuration with no residual magnetization.

DISCUSSION AND CONCLUSION

Important questions about the systems investigated here remain to be explained. They are mainly related to the doubts about if it is really possible to achieve the perfect ice regime in these artificial materials. We must say that if the system with aspect ratio $\gamma_R = \sqrt{3}$ were really in the ice state, then there would be no peak in the specific heat (see Fig.2) but just a smooth bump, because there is no phase transition to the ice state, just a crossover. If it is so, one should not say that this configuration is really degenerate, but just that it is effec-

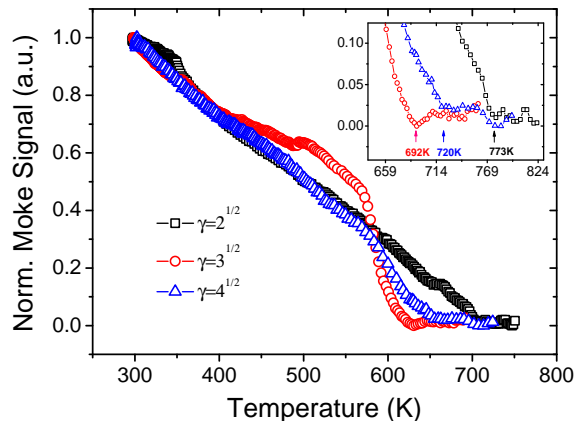


Figure 5. *MOKE* signal as function of temperature for the three lattices compared. Here $T_{\sqrt{2}} \approx 707K$, $T_{\sqrt{3}} \approx 630K$ and $T_{\sqrt{4}} \approx 657K$.

tively degenerate for $T > 0$. However, some details of the theoretical approach and experimental measurements must be observed before any conclusion about a desirable complete and precise description of these artificial compounds. Indeed, γ_R is not a rational number and, therefore, any calculation of the specific heat is not done exactly at the correct value in which the system degenerates. For the simulations, the use of any rational number r very close to $\sqrt{3}$ will imply that the system is only near to the ice regime, but it still keeps some features of the antiferromagnetic (if r is immediately below $\sqrt{3}$) or ferromagnetic phase (if r is immediately above $\sqrt{3}$). Experimentally, things are still more complicated because the measurements of distances between islands have the errors of the instruments and, in addition, the nanoislands are not point dipoles. So, all results concerning the

lattices analyzed are only approximations. Despite these difficulties, our results indicate (theoretically as well as experimentally) that geometry may induce some roles on the thermodynamic properties of these systems.

In conclusion, we have demonstrated experimentally that the lattice geometry can be an important ingredient to transform the thermodynamic properties of artificial spin ice compounds. By stretching the lattice, the fluctuations do not decrease monotonically as expected when the mean distances among the nanoislands increase. Indeed, normally, *ASI* materials are athermal and the spins do not flip easily because a nanoisland contains a large number of atoms. On the other hand, it has been shown that an unambiguous stretching of the square ice may take the system to the ice regime; there is a peculiar rectangular array with aspect ratio $\gamma = \gamma_R = \sqrt{3}$ (rhombic ice), in which the fluctuations become more evident as compared to its counterparts. Note that the nanomagnets constituents of the artificial rhombic ice are akin to the nanomagnets composing all others types of arrays built for this investigation. Therefore, geometry must be important for the different behaviors observed in these systems. The rhombic lattice makes equidistant the four spins meeting at a vertex, similar to the three-dimensional natural and even artificial spin ices[17]. This geometric effect has shown to be more effective in inducing spin fluctuations than the usual way of purely increasing the lattice spacing among the nanoislands. Although all the evidences obtained here suggest that the rhombic ice is in the ice regime, we must be very careful in stating that. To be sure about this, it should be useful to know the behavior of the magnetic structure factor of the moment configurations. If it exhibits the usual pinch singularities, we could assert that the spin ice degeneracy has been really established. Nevertheless, such calculations and/or neutron scattering experiments are out of the scope of the present paper.

-
- [1] Wang, R. F., Nisoli, C., Freitas, R. S., Li, J., McConville, W., Cooley, B. J., Lund, M. S., Samarth, N., Leighton, C., Crespi V. H., and Schiffer, P. Artificial spin ice in a geometrically frustrated lattice of nanoscale ferromagnetic islands. *Nature* **439**, 303 (2006).
 - [2] Möller, G., and Moessner, R. Artificial Square Ice and Related Dipolar Nanoarrays. *Phys. Rev. Lett.* **96**, 237202 (2006).
 - [3] Mól, L.A., Silva, R.L., Silva R.C., Pereira, A.R., Moura-Melo, W.A., and Costa, B.V., *J. Appl. Phys.* **106**, 063913 (2009).
 - [4] Morgan, J.P., Stein, A., Langridge, S., and Marrows, C. Thermal ground-state ordering and elementary excitations in artificial magnetic square ice. *Nature Phys.* **7**, 75 (2011).
 - [5] Silva, R.C., Nascimento, F.S., Mól, L.A. S., Moura-Melo, W.A. and Pereira, A.R. Thermodynamics of elementary excitations in artificial magnetic square ice. *New J. Phys.* **14**, 015008 (2012).
 - [6] Kapaklis, V., Arnalds, U.B., Harman-Clarke, A., apaioannou, E. T., Karimipour, M., Korelis, P., Taroni, A., Holdsworth, P.C.W., Bramwell, S.T., and Hjørvarsson, B. Melting artificial spin ice. *New J. Phys.* **14**, 035009 (2012).
 - [7] Farhan A., Derlet P. M., Kleibert A., Balan A., Chopdekar R. V., Wyss M., Perron J., Scholl A., Nolting F., and Heyderman L. J. Direct Observation of Thermal Relaxation in Artificial Spin Ice. *Phys. Rev. Lett.* **111**, 057204 (2013).
 - [8] Kapaklis V., Arnalds U.B., Farhan A., Chopdekar R.V., Balan A., Scholl A., Heyderman L.J., and Hjørvarsson B. Thermal fluctuations in artificial spin ice. *Nat. Nano.* **9**, 514 (2014).
 - [9] Farhan A., Kleibert A., Derlet P.M., Anghinolfi L., Balan A., Chopdekar R.V., Wyss M., Gliga S., Noltingk F., Heyderman L.J. Thermally induced magnetic relaxation

- in building blocks of artificial. *Phys. Rev. B* **89**, 214405 (2014).
- [10] Farhan A., Derlet P.M., Kleibert A., Balan A., Chopdekar R.V., Wyss M., Anghinolfi L., Nolting F., Heyderman L.J. Exploring hyper-cubic energy landscapes in thermally active finite artificial spin-ice systems. *Nat. Phys.* **9**, 375 (2013).
- [11] Thonig D., Reissaus S., Mertig I., and Henk J. Thermal string excitations in artificial spin-ice square dipolar arrays. *J. Phys.: Condens. Matter* **26** (2014).
- [12] Andersson, M.S., Pappas, S.D., Stopfel, H., Östman, E., Stein, A., Nordblad, P., Mathieu, R., Hjörvarsson, B., and Kapaklis, V. Thermally induced magnetic relaxation in square artificial spin ice. *Scient. Rep.* **6**, 37097 (2016).
- [13] Nascimento, F.S., Mól, L.A.S., Moura-Melo, W.A., and Pereira, A.R. From confinement to deconfinement of magnetic monopoles in artificial rectangular spin ices. *New J. Phys.* **14**, 115019 (2012).
- [14] Ribeiro, I.R.B., Nascimento, F.S., Ferreira, S.O., W.A., Costa C.A.R., Borme, J., Freitas P.P., Wysin, G.M., de Araujo, C.I.L., and Pereira, A.R. Realization of Rectangular Artificial Spin Ice and Direct Observation of High Energy Topology. *Scient. Rep.* **7**, 13982 (2017).
- [15] Nambu, Y. Strings, monopoles, and gauge fields. *Phys. Rev. D* **10**, 4262 (1974).
- [16] Möller, G., and Moessner, R. Magnetic multipole analysis of kagome and artificial spin-ice dipolar arrays *Phys. Rev. B* **80**, 140409(R) (2009).
- [17] Perrin, Y., Canals, B., and Rougemaille, N. Extensive degeneracy, Coulomb phase and magnetic monopoles in artificial square ice. *Nature*, **540**, 410-413 (2016).

ACKNOWLEDGEMENTS

The authors would like to thank the Brazilian agencies CNPq, FAPEMIG and CAPES.